



## Decoding computational complexity: a fractional-order clique-based approach for solving Hilfer fractal-fractional differential equations

Parisa Rahimkhani<sup>1,\*</sup>, Nasrin Samadyar<sup>2</sup>, and Mohsen Razzaghi<sup>3</sup>

<sup>1</sup>Faculty of Science, Mahallat Institute of Higher Education, Mahallat, Iran.

<sup>2</sup>Department of Basic Science, Kermanshah University of Technology, Kermanshah, Iran.

<sup>3</sup>Department of Mathematics and Statistics, Mississippi State University, Mississippi State, Mississippi, USA.

### Abstract

In the current investigation, we propose a novel and computationally efficient numerical framework for solving Hilfer fractal-fractional differential equations (HF-FDEs) by introducing a new class of basis functions termed fractional-order clique functions (FCFs). In contrast to conventional fractional models, which primarily rely on classical kernels and often fall short in encapsulating the intricate interplay between memory-dependent behavior and fractal geometries, the adopted Hilfer fractal-fractional derivative offers a unified formulation that inherently incorporates both non-locality and fractality-features essential for accurately modeling complex real-world processes. To the best of our knowledge, this work marks the first development and implementation of FCFs within a numerical solution framework. The distinctive analytical properties of FCFs facilitate precise, adaptable, and computationally stable representations of HF-FDE solutions. By integrating the FCFs-based approximation with a collocation technique and Newton's iterative algorithm, the under study problem is efficiently transformed into a system of nonlinear algebraic equations. A thorough convergence analysis is presented to ensure the theoretical soundness of the approach, and its practical performance is validated through five numerical examples. The results decisively demonstrate the enhanced accuracy and effectiveness of the proposed method in capturing the multifaceted behavior of fractional dynamic systems when compared to traditional approaches.

**Keywords.** Hilfer fractal-fractional differential equations, Fractional-order clique functions, Convergence analysis, Numerical method.

**1991 Mathematics Subject Classification.** 26A33, 33F05, 65L60.

### 1. INTRODUCTION

Fractional operators can more effectively describe real-world problems in science and engineering compared to classical operators ([1], [8], [19]). This advantage arises from the flexibility of fractional operators to adopt arbitrary orders, whereas classical operators are limited to local derivatives and cannot capture the full memory effect. These equations present significant challenges in obtaining analytical solutions due to the presence of non-integer order derivatives. As a result, considerable attention has been focused on the numerical solutions of different fractional differential equations (FDEs), such as the Chelyshkov wavelets and least squares support vector regression method for FDE arising in optics and engineering [30], the Bell polynomials method for  $\psi$ -fractional integro-differential equations [31], wavelets neural networks approach for  $\psi$ -FDEs [33], finite difference approach for variable-order time fractional diffusion equation [43], the Jacobi polynomials method for the Hadamard fractional Klein-Gordon-Schrödinger equations [15], the generalized Bernoulli polynomials method for nonlinear two-dimensional fractional optimal control problems [11], the Vieta-Fibonacci polynomials method for fractal-fractional differential equations (F-FDEs) system [35], hybrid functions of the Bernstein polynomials and block-pulse functions for optimal control of the nonlinear Volterra integral equations [25], etc.

Received: 07 July 2025 ; Accepted: 19 October 2025.

\* Corresponding author. Email: rahimkhani.parisa@gmail.com, rahimkhani.parisa@mahallat.ac.ir.

In [16] Hilfer introduced a definition of fractional derivative called Hilfer fractional derivative (HFD). The HFD is a generalization of Riemann-Liouville and Caputo fractional derivatives. In fact, the two-parameter family of HFD with order  $\nu$  and  $\gamma$  enables interpolation between the Riemann-Liouville and Caputo derivatives. The type parameter introduces additional types of stationary states and offers an extra degree of freedom in the initial condition. The HFD is a highly effective tool for modeling complex real-world problems due to its enhanced precision. Only a limited number of studies have explored FDEs with HFD, such as Authors in [10] applied the fixed-point method and Mittag-Leffler functions to examine the existence and uniqueness of solutions for FDEs with HFD. Authors in [4] derived sufficient conditions for the existence, uniqueness, and Ulam-Hyers as well as Ulam-Hyers-Rassias stability of FDEs involving HFD. Authors in [45] applied Schaefer's fixed point theorem and the Banach contraction principle to establish existence and uniqueness results for implicit FDEs involving HFD. Authors in [47] investigated the existence of solutions for a nonlocal initial value problem involving FDEs with HFD using fixed-point methods. Authors in [49] examined the existence of solutions for a hybrid fractional differential equation involving the  $\varphi$ -Hilfer derivative with a non-local condition. Authors in [44] used the shifted Legendre polynomials Galerkin method for FDEs involving HFD.

In 2017, Atangana [5] proposed a definition of differential operators that incorporates the convolution of power functions, exponential functions, and generalized Mittag-Leffler function with a fractal derivative. These definitions came to be known as fractal-fractional (FF) differential operators. An FF operator combines the principles of fractional differentiation, known for its non-local properties, with those of the fractal derivative, which exhibits local properties, in a single differentiation. The primary goal of fractal-fractional differentiation is to accurately model fractal dynamics by replacing fractal time with continuous time. Similarly, for a system that is fractal differentiable, the fractal-order derivative is proportional to  $\varphi t^{\varphi-1}$ . It has been highly effective in the mathematical modeling of various scientific fields, including finance [46], biology [42], chaotic different problems [6], etc. This has motivated researchers to develop numerical schemes to obtain approximate solutions for such problems. For example, the generalized Lucas wavelets method for FF optimal control problems [38], the Müntz-Legendre polynomials method for FF 2D optimal control problems [36], the shifted Chebyshev cardinal functions method for the FF Schrödinger equations [12], the shifted Vieta-Fibonacci polynomials method for the FF fifth-order KdV equation [13], the fractional shifted Morgan-Voyce neural networks method for FF pantograph differential equations [32], artificial neural networks method for variable-order FF Mittag-Leffler differential equations [50], and piecewise Lagrange interpolation method of fractal fractional model of tumor-immune interaction with two different kernels [40].

Recently, Shloof et al. [41] introduced a novel concept of differentiation, known as HF-FDEs, which integrates both fractal effects and memory. They obtained Hilfer fractal-fractional (HFF) derivative operational matrix of the shifted Legendre polynomials for solving introduced differential equations. Due to the application of this problem and the lack of other works in this field, we decided to solve these problems numerically. For solving HFF differential equations, we introduce and then apply FCFs. It is worth mentioning here that a small number of FCFs is needed to achieve a reliable approximate solution, also, simulation results demonstrate that the obtained solution is practical.

It is noteworthy that clique polynomials (CPs), originally introduced by Hoede and Li, are intrinsically connected to the maximum clique problem (MCP) [17, 18]. The MCP represents a fundamental challenge in combinatorial optimization, with broad applicability across various disciplines, including economics, classification theory, scheduling, information retrieval, biomedical engineering, and signal transmission analysis. Due to their structural properties, CPs have found extensive utility in the development of advanced numerical methods for solving a wide range of differential equations. Notable applications include time-fractional Klein-Gordon equation [9], classical Klein-Gordon equation [22], fractional partial differential equations [2], boundary-layer natural convection flow problem [21], multi-delay fractional differential equations [27], space-time fractional Schrödinger equation [14], fractional-order Brusselator chemical model [20], and distributed-order fractional ordinary differential equations [26].

Arrangement of the article: In section 2, we recall some important definitions related to fractional, Hilfer, FF, and HFF definitions. In Section 3, FCFs are defined. Section 4 discusses the FCFs-based numerical scheme for solving HF-FDEs. Section 5 shows the convergence of the presented method. Section 6 covers the numerical applications and the discussion of results. Finally, section 7 presents the findings and concludes of the paper.



2. FUNDAMENTALS AND KEY DEFINITIONS

2.1. Fractional definitions.

**Definition 2.1.** The Riemann-Liouville fractional integral of order  $\nu > 0$ , is obtained as [41]

$$I_{a^+}^\nu R(t) = \frac{1}{\Gamma(\nu)} \int_a^t (t - \vartheta)^{\nu-1} R(\vartheta) d\vartheta, \quad t > a. \tag{2.1}$$

**Definition 2.2.** The Riemann-Liouville fractional derivative of order  $\nu > 0$ , is obtained as [41]

$${}^R D_{a^+}^\nu R(t) = \frac{1}{\Gamma(n - \nu)} \left( \frac{d^n}{dt^n} \int_a^t (t - \vartheta)^{n-\nu-1} R(\vartheta) d\vartheta \right), \quad t > a \geq 0, n - 1 < \nu \leq n. \tag{2.2}$$

**Definition 2.3.** The Caputo fractional derivative of order  $\nu > 0$ , is obtained as [41]

$${}^C D_{a^+}^\nu R(t) = \frac{1}{\Gamma(n - \nu)} \int_a^t (t - \vartheta)^{n-\nu-1} R(\vartheta) d\vartheta, \quad t > a \geq 0, n - 1 < \nu \leq n. \tag{2.3}$$

**Corollary 2.4.** The Caputo fractional derivative of  $t^\alpha$  is given [34]

$${}^C D^\nu t^\alpha = \frac{\Gamma(\alpha + 1)}{\Gamma(\alpha - \nu + 1)} t^{\alpha-\nu}, \quad \alpha > \nu. \tag{2.4}$$

2.2. Hilfer and fractal-fractional definitions.

**Definition 2.5.** The Hilfer fractional derivative of function  $R(t)$  is given as [41]

$$D_{a^+}^{\nu,\gamma} R(t) = (I_{a^+}^{\gamma(1-\nu)} \frac{d}{dt} (I_{a^+}^{(1-\gamma)(1-\nu)} R(t))), \quad 0 < \nu \leq 1, 0 \leq \gamma \leq 1. \tag{2.5}$$

In particular case, if  $\gamma = 0$  and  $\gamma = 1$ , then Hilfer derivative reduced to Riemann-Liouville Eq. (2.2) and Caputo fractional derivative Eq. (2.3).

**Definition 2.6.** Let  $R(t)$  be differentiable on  $(a, b)$ . If  $R(t)$  is fractally differentiable of order  $\wp$  on  $(a, b)$ , then the FF derivative in Caputo sense with power law kernel of the function  $R(t)$  is defined of order  $\nu$  and  $\wp$  is given as [41]

$${}^C D_{a^+}^{\nu,\wp} R(t) = \frac{1}{\Gamma(n - \nu)} \int_a^t (t - \vartheta)^{n-\nu-1} \frac{dR(\vartheta)}{d\vartheta^\wp} d\vartheta, \tag{2.6}$$

where

$$\frac{dR}{dt^\wp} = \lim_{t \rightarrow \vartheta} \frac{R(t) - R(\vartheta)}{t^\wp - \vartheta^\wp} = \frac{1}{\wp t^{\wp-1}} \frac{d}{dt} R(t), \quad 0 < n - 1 < \nu, \wp \leq n.$$

**Definition 2.7.** Let  $R(t)$  be differentiable on  $(a, b)$ . If  $R(t)$  is fractally differentiable of order  $\wp$  on  $(a, b)$ , then the FF derivative in Riemann-Liouville sense with power law kernel of the function  $R(t)$  of order  $\nu$  and  $\wp$  is given as [41]

$${}^R D_{a^+}^{\nu,\wp} R(t) = \frac{1}{\Gamma(n - \nu)} \frac{d}{ds^\wp} \int_a^t (t - \vartheta)^{n-\nu-1} R(\vartheta) d\vartheta. \tag{2.7}$$

**Definition 2.8.** Assume that  $R(t)$  is continuous in  $(a, b)$ . Then the FF integral in Riemann-Liouville sense of order  $\nu$  and  $\wp$  is given as [41]

$$I_{a^+}^{\nu,\wp} R(t) = \frac{\wp}{\Gamma(\nu)} \int_a^t \vartheta^{\wp-1} (t - \vartheta)^{\nu-1} R(\vartheta) d\vartheta, \quad t > a. \tag{2.8}$$

**Corollary 2.9.** The Hilfer fractional derivative of  $t^\alpha$  is given [41]

$$D^{\gamma,\wp} t^\alpha = \frac{\Gamma(\alpha + 1)}{\Gamma(\alpha - \gamma + 1)} t^{\alpha-\gamma}, \quad 0 < \gamma, \wp \leq 1. \tag{2.9}$$



### 2.3. Hilfer fractal-fractional definitions.

**Definition 2.10.** Let  $R : [a, b] \rightarrow \mathbb{R}$ ,  $0 < \nu \leq 1$ ,  $0 \leq \gamma \leq 1$  is a continuous function on  $[a, b]$  and fractal differentiable on  $(a, b)$  with order  $\wp$ , then the HFF derivative of function  $R(t)$  is given as [41]

$$D_{a^+}^{\nu, \gamma, \wp} R(t) = (I_{a^+}^{\gamma(1-\nu)} \frac{d}{dt^\wp} (I_{a^+}^{(1-\gamma)(1-\nu)} R(t))), \quad (2.10)$$

where

$$\frac{dR}{dt^\wp} = \lim_{t \rightarrow \vartheta} \frac{R(t) - R(\vartheta)}{t^\wp - \vartheta^\wp}.$$

**Remark 2.11.** If  $\gamma = 0$ , we have

$$D_{a^+}^{\nu, 0, \wp} R(t) = \frac{d}{dt^\wp} (I_{a^+}^{(1-\nu)} R(t)),$$

also for  $\gamma = 1$ , we yield

$$D_{a^+}^{\nu, 1, \wp} R(t) = I_{a^+}^{(1-\nu)} \frac{d}{dt^\wp} (R(t)).$$

**Corollary 2.12.** The HFF derivative of  $t^\alpha$  is given [41]

$$D^{\nu, \gamma, \wp} t^\alpha = \frac{\Gamma(\alpha + 1)}{\wp \Gamma(\alpha - \nu + 1)} t^{\alpha - \nu + 1 - \wp}, \quad \nu, \gamma, \wp \in (0, 1). \quad (2.11)$$

### 3. FRACTIONAL-ORDER CLIQUE FUNCTIONS

The CP of a graph  $\mathcal{G}$ , denoted by  $\mathfrak{C}(\mathcal{G}, t)$ , is formally defined as follows [9]:

$$\mathfrak{C}(\mathcal{G}, t) = \sum_{r=0}^i \beta_r(\mathcal{G}) t^r, \quad \beta_0(\mathcal{G}) = 1. \quad (3.1)$$

Here,  $\beta_r(\mathcal{G})$  denotes the number of  $r$ -cliques in the graph  $\mathcal{G}$ . In particular, the CP of a complete graph  $\mathbf{H}_i$  with  $i$  vertices is given by [9]:

$$\mathfrak{C}(\mathbf{H}_i, t) = (1 + t)^i = \sum_{r=0}^i \binom{i}{r} t^r.$$

We now proceed to define the FCFs over the closed interval  $[0, 1]$  as follows:

$$\mathfrak{C}(\mathbf{H}_i, t, \lambda) = \sum_{r=0}^i \binom{i}{r} t^{r\lambda}. \quad (3.2)$$

Any function  $R(t) \in L^2[0, 1]$  can be approximated with high accuracy using the FCFs, expressed as follows:

$$R(t) \simeq R^*(t) = \sum_{j=0}^M a_j \mathfrak{C}(\mathbf{H}_j, t, \lambda) = A^T \mathfrak{C}(t), \quad (3.3)$$

where

$$A = [a_0, a_1, \dots, a_M]^T.$$

$$\mathfrak{C}(t) = [\mathfrak{C}(\mathbf{H}_0, t, \lambda), \mathfrak{C}(\mathbf{H}_1, t, \lambda), \dots, \mathfrak{C}(\mathbf{H}_M, t, \lambda)]^T.$$

By utilizing Equation (3.3), we obtain the following result:

$$A = \mathfrak{Q}^{-1} \langle R(t), \mathfrak{C}(t) \rangle,$$

where  $\mathfrak{Q} = \langle \mathfrak{C}(t), \mathfrak{C}(t) \rangle$ , and  $\langle \cdot, \cdot \rangle$  denotes the standard inner product between two arbitrary functions.



4. IMPLEMENTATION OF THE PROPOSED TECHNIQUE

In this article, we will numerically solve the following HF-FDEs using the FCFs:

$$D^{\nu,\gamma,\varphi}R(t) = \mathcal{F}(t, R(t), {}^C\mathcal{D}^\nu R(t), D^{\nu,\gamma}R(t)). \tag{4.1}$$

The initial condition is given as follows:

$$\text{if } \gamma = 0, \quad R(0) = R_0,$$

also if  $0 < \gamma < 1$ ,  $I^{(1-\gamma)(1-\nu),\varphi}R(t)|_{t=0} = R_0$ .

For solving Eq. (4.1), the unknown function  $R(t)$  is approximated as

$$R(t) \simeq R_0 + t \left( \sum_{j=0}^M a_j \mathfrak{C}(\mathbf{H}_j, t, \lambda) \right) = R^*(t). \tag{4.2}$$

By applying Corollary 2.4 and Eq. (3.2), the Caputo fractional derivative function ( ${}^C\mathcal{D}^\nu R(t)$ ) is approximated as

$$\begin{aligned} {}^C\mathcal{D}^\nu R(t) &\simeq \sum_{j=0}^M \sum_{r=0}^j a_j \binom{j}{r} {}^C\mathcal{D}^\nu (t^{r\lambda+1}) \\ &= \sum_{j=0}^M \sum_{r=0}^j a_j \binom{j}{r} \frac{\Gamma(r\lambda+2)}{\Gamma(r\lambda+2-\nu)} t^{r\lambda+1-\nu} = {}^C\mathcal{D}^\nu R^*(t). \end{aligned} \tag{4.3}$$

From Corollary 2.9 and Eq. (3.2), the Hilfer fractional derivative function ( $D^{\nu,\gamma}R(t)$ ) is approximated as

$$\begin{aligned} D^{\nu,\gamma}R(t) &\simeq \sum_{j=0}^M \sum_{r=0}^j a_j \binom{j}{r} D^{\nu,\gamma} (t^{r\lambda+1}) \\ &= \sum_{j=0}^M \sum_{r=0}^j a_j \binom{j}{r} \frac{\Gamma(r\lambda+2)}{\Gamma(r\lambda+2-\nu)} t^{r\lambda+1-\nu} = D^{\nu,\gamma}R^*(t). \end{aligned} \tag{4.4}$$

By considering Corollary 2.12 and Eq. (3.2), the HFF derivative function ( $D^{\nu,\gamma,\varphi}R(t)$ ) is approximated as

$$\begin{aligned} D^{\nu,\gamma,\varphi}R(t) &\simeq \sum_{j=0}^M \sum_{r=0}^j a_j \binom{j}{r} D^{\nu,\gamma,\varphi} (t^{r\lambda+1}) \\ &= \sum_{j=0}^M \sum_{r=0}^j a_j \binom{j}{r} \frac{\Gamma(r\lambda+2)}{\varphi\Gamma(r\lambda+2-\nu)} t^{r\lambda+2-\nu-\varphi} = D^{\nu,\gamma,\varphi}R^*(t). \end{aligned} \tag{4.5}$$

Now, we can write

$$I^{(1-\gamma)(1-\nu),\varphi}R(t) \simeq I^{(1-\gamma)(1-\nu),\varphi}R_0 + I^{(1-\gamma)(1-\nu),\varphi}t \left( \sum_{j=0}^M a_j \mathfrak{C}(\mathbf{H}_j, t, \lambda) \right). \tag{4.6}$$

Using the definition of FF integral in (2.8), we get

$$\begin{aligned} I^{(1-\gamma)(1-\nu),\varphi}R_0 &= \frac{\varphi R_0}{\Gamma((1-\gamma)(1-\nu))} \int_0^t s^{\varphi-1} (t-s)^{(1-\gamma)(1-\nu)-1} ds \\ &= \frac{\varphi R_0}{\Gamma((1-\gamma)(1-\nu))} \int_0^t t^{\varphi-1} \left(\frac{s}{t}\right)^{\varphi-1} t^{(1-\gamma)(1-\nu)-1} \left(1-\frac{s}{t}\right)^{(1-\gamma)(1-\nu)-1} t d\frac{s}{t} \\ &= \frac{\varphi R_0}{\Gamma((1-\gamma)(1-\nu))} t^{(1-\gamma)(1-\nu)+\varphi-1} \frac{\Gamma(\varphi)\Gamma((1-\gamma)(1-\nu))}{\Gamma(\varphi+(1-\gamma)(1-\nu))} \mathcal{I}(1; \varphi, (1-\gamma)(1-\nu)), \end{aligned} \tag{4.7}$$



and

$$\begin{aligned}
I^{(1-\gamma)(1-\nu),\wp} t^{r\lambda+1} &= \frac{\wp}{\Gamma((1-\gamma)(1-\nu))} \int_0^t s^{\wp+r\lambda} (t-s)^{(1-\gamma)(1-\nu)-1} ds \\
&= \frac{\wp}{\Gamma((1-\gamma)(1-\nu))} \int_0^t t^{\wp+r\lambda} \left(\frac{s}{t}\right)^{\wp+r\lambda} t^{(1-\gamma)(1-\nu)-1} \left(1-\frac{s}{t}\right)^{(1-\gamma)(1-\nu)-1} t d\frac{s}{t} \\
&= \frac{\wp}{\Gamma((1-\gamma)(1-\nu))} t^{\wp+r\lambda+(1-\gamma)(1-\nu)} \frac{\Gamma(\wp+r\lambda+1)\Gamma((1-\gamma)(1-\nu))}{\Gamma(\wp+r\lambda+1+(1-\gamma)(1-\nu))} \\
&\quad \times \mathcal{I}(1; \wp+r\lambda+1, (1-\gamma)(1-\nu)), \tag{4.8}
\end{aligned}$$

where  $\mathcal{I}(t; a, b)$  is the regularized beta function [28].

From Eqs. (4.6)-(4.8), we achieve

$$\begin{aligned}
I^{(1-\gamma)(1-\nu),\wp} R(t) &\simeq \frac{\wp R_0}{\Gamma((1-\gamma)(1-\nu))} t^{(1-\gamma)(1-\nu)+\wp-1} \frac{\Gamma(\wp)\Gamma((1-\gamma)(1-\nu))}{\Gamma(\wp+(1-\gamma)(1-\nu))} \mathcal{I}(1; \wp, (1-\gamma)(1-\nu)) \\
&\quad + \sum_{j=0}^M \sum_{r=0}^j a_j \binom{j}{r} \frac{\wp}{\Gamma((1-\gamma)(1-\nu))} t^{\wp+r\lambda+(1-\gamma)(1-\nu)} \frac{\Gamma(\wp+r\lambda+1)\Gamma((1-\gamma)(1-\nu))}{\Gamma(\wp+r\lambda+1+(1-\gamma)(1-\nu))} \\
&\quad \times \mathcal{I}(1; \wp+r\lambda+1, (1-\gamma)(1-\nu)) = I^{(1-\gamma)(1-\nu),\wp} R^*(t). \tag{4.9}
\end{aligned}$$

We introduce the residual error function ( $Res(t)$ ) as follows

$$Res(t) = D^{\nu,\gamma,\wp} R^*(t) - \mathcal{F}(t, R^*(t), {}^C D^\nu R^*(t), D^{\nu,\gamma} R^*(t)), \tag{4.10}$$

For  $\gamma = 0$ , by collocating the obtained algebraic equation at the zeros of the shifted Legendre polynomials ( $P_M(t)$ ), we get

$$Res(t_i) = 0, \quad i = 1, 2, \dots, M. \tag{4.11}$$

For  $0 < \gamma < 1$ , we collocate Eq. (4.10) and consider Eq. (4.9), we get

$$\begin{cases} Res(t_i) = 0, & i = 1, 2, \dots, M-1, \\ I^{(1-\gamma)(1-\nu),\wp} R^*(t)|_{t=0} = R_0. \end{cases} \tag{4.12}$$

Finally, we obtain a system of  $M$  algebraic equations with  $M$  unknowns. The above system should be solved to determine  $a_i, i = 1, 2, \dots, M$ . To this end, Newton's iterative scheme is employed, and the FindRoot package in Mathematica software is utilized for its implementation.

## 5. CONVERGENCE ANALYSIS OF THE CURRENT SCHEME

The purpose of this section is to evaluate the convergence of the current algorithm within the Sobolev space. The Sobolev norm of integer order  $\mu \geq 0$  on the interval  $(0, 1)$  is defined as [32]

$$\|R\|_{H^\mu(0,1)} = \left( \sum_{j=0}^{\mu} \int_0^1 |R^{(j)}(t)| dt \right)^{\frac{1}{2}} = \left( \sum_{j=0}^{\mu} \|R^{(j)}(t)\|_{L^2(0,1)}^2 \right)^{\frac{1}{2}}, \tag{5.1}$$

where  $R^{(j)}$  indicates the distributional derivative of order  $j$  of  $R$ .

**Theorem 5.1.** *Let  $R \in H^\mu(0, 1)$  with  $\mu \geq 0$  and  $M \geq \mu$ , and let  $R^*$  represent the best approximation of  $R$  obtained using the FCFs. Then, the following inequality holds [32]:*

$$\|R - R^*\|_{L^2(0,1)} \leq \zeta \Delta M^{-s}, \tag{5.2}$$

and for  $1 \leq s \leq \mu$  we yield

$$\|R - R^*\|_{H^s(0,1)} \leq \zeta \Delta M^{2s-\frac{1}{2}-\tau}, \tag{5.3}$$



where  $\Delta = \|R^{(\mu)}\|_{L^2(0,1)}$ .

**Lemma 5.2.** *If  $R^*(t)$  represents the best approximation to  $R(t)$  within the space spanned by the FCFs, then we have the following inequality*

$$\|I^\nu R - I^\nu R^*\|_{L^2[0,1]} \leq \ell_1 \|R - R^*\|_{L^2[0,1]}, \tag{5.4}$$

where  $\ell_1 = \frac{1}{\Gamma(\nu)\sqrt{2\nu(2\nu-1)}}$ .

*Proof.* Using Eq. (2.1), we derive the following relation:

$$I^\nu R(t) - I^\nu R^*(t) = \frac{1}{\Gamma(\nu)} \int_0^t (t-\vartheta)^{\nu-1} (R(\vartheta) - R^*(\vartheta)) d\vartheta. \tag{5.5}$$

By the Schwarz's inequality, we get

$$\begin{aligned} |I^\nu R(t) - I^\nu R^*(t)| &\leq \frac{1}{\Gamma(\nu)} \left( \int_0^t (t-\vartheta)^{2\nu-2} d\vartheta \right)^{\frac{1}{2}} \left( \int_0^t (R(\vartheta) - R^*(\vartheta))^2 d\vartheta \right)^{\frac{1}{2}} \\ &\leq \frac{1}{\Gamma(\nu)\sqrt{(2\nu-1)}} t^{\nu-\frac{1}{2}} \|R - R^*\|_{L^2[0,1]}. \end{aligned} \tag{5.6}$$

Applying the  $L^2$ -norm to both sides of Eq. (5.6), we obtain the desired result:

$$\begin{aligned} \|I^\nu R - I^\nu R^*\|_{L^2[0,1]} &\leq \frac{1}{\Gamma(\nu)\sqrt{(2\nu-1)}} \|t^{\nu-\frac{1}{2}}\|_{L^2[0,1]} \|R - R^*\|_{L^2[0,1]} \\ &\leq \frac{1}{\Gamma(\nu)\sqrt{2\nu(2\nu-1)}} \|R - R^*\|_{L^2[0,1]}. \end{aligned} \tag{5.7}$$

□

**Lemma 5.3.** *Assuming the conditions of Lemma 5.2, we obtain the following inequality:*

$$\|\mathcal{D}^\nu R - \mathcal{D}^\nu R^*\|_{L^2[0,1]} \leq \ell_2 \|R - R^*\|_{L^2[0,1]}, \tag{5.8}$$

where  $\ell_2 = \frac{1}{\Gamma(n-\nu)\sqrt{(2n-2\nu)(2n-2\nu-1)}}$ .

*Proof.* The proof follows similarly to that of Lemma 5.2.

□

**Lemma 5.4.** *If  $R^*(t)$  denotes the best approximation to  $R(t)$  within the space spanned by the FCFs, that  $R(t), R^*(t) \in L[0, 1]$ , then we derive*

$$\|\mathcal{D}^{\nu,\gamma} R - \mathcal{D}^{\nu,\gamma} R^*\|_{L^2[0,1]} \leq \ell_3 \|R - R^*\|_{L^2[0,1]}, \tag{5.9}$$

where  $\ell_3 = \frac{1}{2\Gamma(\gamma(1-\nu))\Gamma((1-\gamma)(1-\nu))\sqrt{\gamma(1-\nu)(2\gamma(1-\nu)-1)(1-\gamma)(1-\nu)(2(1-\gamma)(1-\nu)-1)}}$ .

*Proof.* From Eq. (2.5), we get

$$\mathcal{D}^{\nu,\gamma} R(t) - \mathcal{D}^{\nu,\gamma} R^*(t) = (I^{\gamma(1-\nu)} \frac{d}{dt} (I^{(1-\gamma)(1-\nu)} R(t))) - (I^{\gamma(1-\nu)} \frac{d}{dt} (I^{(1-\gamma)(1-\nu)} R^*(t))). \tag{5.10}$$



Taking the  $H^s$ -norm to both sides of Eq. (5.10), Lemma 5.2 and the definition of the Sobolev space, we conclude

$$\begin{aligned}
\|\mathcal{D}^{\nu,\gamma}R - \mathcal{D}^{\nu,\gamma}R^*\|_{L^2[0,1]} &\leq \|(I^{\gamma(1-\nu)} \frac{d}{dt}(I^{(1-\gamma)(1-\nu)}R(t))) - (I^{\gamma(1-\nu)} \frac{d}{dt}(I^{(1-\gamma)(1-\nu)}R^*(t)))\|_{L^2[0,1]} \\
&\leq \frac{1}{\Gamma(\gamma(1-\nu))\sqrt{2\gamma(1-\nu)(2\gamma(1-\nu)-1)}} \\
&\times \|\frac{d}{dt}(I^{(1-\gamma)(1-\nu)}R(t) - I^{(1-\gamma)(1-\nu)}R^*(t))\|_{L^2[0,1]} \\
&\leq \frac{1}{\Gamma(\gamma(1-\nu))\sqrt{2\gamma(1-\nu)(2\gamma(1-\nu)-1)}} \\
&\times \|I^{(1-\gamma)(1-\nu)}R(t) - I^{(1-\gamma)(1-\nu)}R^*(t)\|_{H^s[0,1]} \\
&\leq \frac{1}{\Gamma(\gamma(1-\nu))\sqrt{2\gamma(1-\nu)(2\gamma(1-\nu)-1)}} \\
&\times \frac{1}{\Gamma((1-\gamma)(1-\nu))\sqrt{2(1-\gamma)(1-\nu)(2(1-\gamma)(1-\nu)-1)}} \\
&\times \|R - R^*\|_{L^2[0,1]}. \tag{5.11}
\end{aligned}$$

□

**Lemma 5.5.** *If the function  $R(t)$  and  $R^*(t)$  are continuous and fractal differentiable on  $(0, 1)$  with order  $\wp$ , we have*

$$\left\| \frac{dR(t)}{dt^\wp} - \frac{dR^*(t)}{dt^\wp} \right\|_{L^2[0,1]} \leq \frac{1}{\wp\sqrt{3-2\wp}} \|R - R^*\|_{H^s[0,1]}. \tag{5.12}$$

*Proof.* Using Ref. [37], we can write

$$\frac{dR(t)}{dt^\wp} - \frac{dR^*(t)}{dt^\wp} = \frac{1}{\wp t^{\wp-1}} \left( \frac{dR(t)}{dt} - \frac{dR^*(t)}{dt} \right). \tag{5.13}$$

Applying the  $L^2$ -norm to both sides of Eq. (5.13) and the definition of the Sobolev space, we acquire

$$\begin{aligned}
\left\| \frac{dR(t)}{dt^\wp} - \frac{dR^*(t)}{dt^\wp} \right\|_{L^2[0,1]} &\leq \frac{1}{\wp} \|t^{1-\wp}\|_{L^2[0,1]} \left\| \frac{dR(t)}{dt} - \frac{dR^*(t)}{dt} \right\|_{L^2[0,1]} \\
&\leq \frac{1}{\wp\sqrt{3-2\wp}} \|R - R^*\|_{H^s[0,1]}. \tag{5.14}
\end{aligned}$$

□

**Lemma 5.6.** *Assume the assumptions of Lemma 5.4 hold, then we attain*

$$\|\mathcal{D}^{\nu,\gamma,\wp}R - \mathcal{D}^{\nu,\gamma,\wp}R^*\|_{L^2[0,1]} \leq \ell_4 \|R - R^*\|_{L^2[0,1]}, \tag{5.15}$$

where

$$\ell_4 = \frac{1}{2\wp\Gamma(\gamma(1-\nu))\Gamma((1-\gamma)(1-\nu))\sqrt{\gamma(1-\nu)(2\gamma(1-\nu)-1)(3-2\wp)(1-\gamma)(1-\nu)(2(1-\gamma)(1-\nu)-1)}}.$$



*Proof.* Considering Eq. (2.10) and Lemmas 5.2 and 5.5, we derive

$$\begin{aligned}
 \|\mathcal{D}^{\nu,\gamma,\wp} R - \mathcal{D}^{\nu,\gamma,\wp} R^*\|_{L^2[0,1]} &\leq \|(I^{\gamma(1-\nu)} \frac{d}{dt^\wp} (I^{(1-\gamma)(1-\nu)} R(t))) \\
 &\quad - (I^{\gamma(1-\nu)} \frac{d}{dt^\wp} (I^{(1-\gamma)(1-\nu)} R^*(t)))\|_{L^2[0,1]} \\
 &\leq \frac{1}{\Gamma(\gamma(1-\nu))\sqrt{2\gamma(1-\nu)(2\gamma(1-\nu)-1)}} \\
 &\quad \times \|\frac{d}{dt^\wp} (I^{(1-\gamma)(1-\nu)} R(t) - I^{(1-\gamma)(1-\nu)} R^*(t))\|_{L^2[0,1]} \\
 &\leq \frac{1}{\wp\Gamma(\gamma(1-\nu))\sqrt{2\gamma(1-\nu)(2\gamma(1-\nu)-1)(3-2\wp)}} \\
 &\quad \times \|I^{(1-\gamma)(1-\nu)} R(t) - I^{(1-\gamma)(1-\nu)} R^*(t)\|_{H^s[0,1]} \\
 &\leq \frac{1}{\wp\Gamma(\gamma(1-\nu))\sqrt{2\gamma(1-\nu)(2\gamma(1-\nu)-1)(3-2\wp)}} \\
 &\quad \times \frac{1}{\Gamma((1-\gamma)(1-\nu))\sqrt{2(1-\gamma)(1-\nu)(2(1-\gamma)(1-\nu)-1)}} \\
 &\quad \times \|R - R^*\|_{L^2[0,1]}. \tag{5.16}
 \end{aligned}$$

□

**Theorem 5.7.** *If we employ the FCFs to approximate the HFF derivative in the HF-FDEs, and assume that the Lipschitz conditions for the function  $\mathcal{F}$  with constants  $\eta_i, i = 1, 2, 3$ , we can converge to its exact solution.*

*Proof.* Using Eq. (4.1), we get the error of the presented method as

$$\begin{aligned}
 \|Error\|_{L^2[0,1]} &\leq \|D^{\nu,\gamma,\wp} R - \mathcal{F}(., R, {}^C\mathcal{D}^\nu R, D^{\nu,\gamma} R) \\
 &\quad - D^{\nu,\gamma,\wp} R^* + \mathcal{F}(., R^*, {}^C\mathcal{D}^\nu R^*, D^{\nu,\gamma} R^*)\|_{L^2[0,1]} \\
 &\leq \|D^{\nu,\gamma,\wp} R - D^{\nu,\gamma,\wp} R^*\|_{L^2[0,1]} \\
 &\quad + \eta_1 \|R - R^*\|_{L^2[0,1]} \\
 &\quad + \eta_2 \|{}^C\mathcal{D}^\nu R - {}^C\mathcal{D}^\nu R^*\|_{L^2[0,1]} \\
 &\quad + \eta_3 \|D^{\nu,\gamma} R - D^{\nu,\gamma} R^*\|_{L^2[0,1]} \\
 &\leq (\ell_4 + \eta_1 + \eta_2\ell_2 + \eta_3\ell_3) \|R - R^*\|_{L^2[0,1]}. \tag{5.17}
 \end{aligned}$$

$$\|Error\|_{L^2[0,1]} \leq (\ell_4 + \eta_1 + \eta_2\ell_2 + \eta_3\ell_3)\zeta\Delta M^{-s}. \tag{5.18}$$

It is clear from Eq. (5.18) that as  $M \rightarrow \infty$ , then  $\|Error\|_{L^2[0,1]} \rightarrow 0$ . This indicates that the developed method is convergent. □

## 6. NUMERICAL RESULTS

In this section, we demonstrate the efficiency and precision of the proposed scheme by solving five numerical examples and presenting the results through figures and tables. When the exact solution to the problem is known, the absolute error serves as a means of evaluating the accuracy and reliability of the proposed method. Conversely, when the exact solution is unknown, the residual error ( $|Res(t_i)|$ ) is employed to assess the accuracy of the results.

**Example 6.1.** Consider the following HF-FDE as [41]:

$$D^{\nu,\gamma,\wp} R(t) = 1 - R^2(t), \tag{6.1}$$



with the initial conditions

$$\begin{cases} R(0) = 0, & \gamma = 0, \\ I^{(1-\gamma)(1-\nu),\varphi} R(t)|_{t=0} = 0, & 0 < \gamma < 1. \end{cases}$$

The exact solution of the classical model is  $R(t) = \frac{e^{2t}-1}{e^{2t}+1}$ . Table 1 lists the numerical results (NRs) and absolute errors (AEs) for  $\nu = \gamma = \varphi = 1, \lambda = \frac{1}{2}$ , and  $M = 15$ . In fact, in this table, we compare our results with the trigonometric basic functions (TBFs) [3], and Legendre operational matrix (LOM) [41]. Table 2 reports the AEs values for distinct values of  $M$ . This table shows that the AE decrease with the increase of  $M$ . The NRs and residual error (REs) for  $\lambda = \frac{1}{2}$ , and varied values of  $\nu, \gamma, \varphi, M$  are shown in Table 3.

TABLE 1. The NRs and AEs for  $\nu = \gamma = \varphi = 1, \lambda = \frac{1}{2}$ , and  $M = 15$  (Example 6.1).

$t$	<i>Exact solution</i>	<i>NRs</i>			<i>AEs</i>		
		<i>TBF</i>	<i>LOM</i>	<i>Presented method</i>	<i>TBF</i>	<i>LOM</i>	<i>Presented method</i>
0.0	0.0000000000	0.000000	0.0000000000	0.0000000000	0	$1.08 \times 10^{-10}$	0
0.2	0.1973753202	0.197773	0.1973753208	0.1973753578	$3.98 \times 10^{-4}$	$3.76 \times 10^{-8}$	$3.76 \times 10^{-8}$
0.4	0.3799489623	0.380422	0.3799489608	0.3799489865	$4.73 \times 10^{-4}$	$3.66 \times 10^{-8}$	$2.42 \times 10^{-8}$
0.6	0.5370495670	0.537449	0.5370495562	0.5370495759	$3.99 \times 10^{-4}$	$3.00 \times 10^{-8}$	$8.90 \times 10^{-9}$
0.8	0.6640367703	0.664285	0.6640367336	0.6640367692	$2.48 \times 10^{-4}$	$3.00 \times 10^{-8}$	$1.03 \times 10^{-9}$
1.0	0.7615941560	0.761671	0.7615941295	0.7615941567	$7.68 \times 10^{-5}$	$2.65 \times 10^{-8}$	$7.79 \times 10^{-10}$

TABLE 2. The AEs for  $\nu = \gamma = \varphi = 1, \lambda = \frac{1}{2}$ , and varied values of  $M$  (Example 6.1).

$t$	$M = 6$	$M = 8$	$M = 10$	$M = 14$	$M = 15$
0.0	0	0	0	0	0
0.2	$1.27 \times 10^{-4}$	$3.15 \times 10^{-5}$	$5.85 \times 10^{-6}$	$3.71 \times 10^{-7}$	$3.76 \times 10^{-8}$
0.4	$1.18 \times 10^{-4}$	$2.72 \times 10^{-5}$	$5.22 \times 10^{-6}$	$3.30 \times 10^{-7}$	$2.42 \times 10^{-8}$
0.6	$9.71 \times 10^{-5}$	$2.27 \times 10^{-5}$	$4.34 \times 10^{-6}$	$2.74 \times 10^{-7}$	$8.90 \times 10^{-9}$
0.8	$7.65 \times 10^{-5}$	$1.79 \times 10^{-5}$	$3.41 \times 10^{-6}$	$2.14 \times 10^{-7}$	$1.03 \times 10^{-9}$
1.0	$5.75 \times 10^{-5}$	$1.34 \times 10^{-5}$	$2.56 \times 10^{-6}$	$1.62 \times 10^{-7}$	$7.79 \times 10^{-10}$

TABLE 3. The NRs and REs for  $\lambda = \frac{1}{2}$ , and varied values of  $\nu, \gamma, \varphi, M$  (Example 6.1).

$t$	$M = 7; \nu = \gamma = \varphi = 0.7$		$M = 8; \nu = \gamma = \varphi = 0.8$		$M = 9; \nu = \gamma = \varphi = 0.9$		$M = 10; \nu = \gamma = \varphi = 1$	
	<i>NRs</i>	<i>REs</i>	<i>NRs</i>	<i>REs</i>	<i>NRs</i>	<i>REs</i>	<i>NRs</i>	<i>REs</i>
0.1	0.358664	$4.96 \times 10^{-4}$	0.248088	$1.14 \times 10^{-3}$	0.160773	$2.38 \times 10^{-4}$	0.099662	$7.01 \times 10^{-6}$
0.2	0.456068	$2.25 \times 10^{-3}$	0.366105	$7.40 \times 10^{-5}$	0.275240	$3.83 \times 10^{-5}$	0.197369	$1.33 \times 10^{-6}$
0.4	0.561341	$1.24 \times 10^{-4}$	0.516822	$8.40 \times 10^{-5}$	0.452971	$3.13 \times 10^{-6}$	0.379944	$1.69 \times 10^{-7}$
0.6	0.621476	$5.53 \times 10^{-5}$	0.612773	$3.10 \times 10^{-4}$	0.583597	$9.44 \times 10^{-7}$	0.537045	$5.15 \times 10^{-8}$
0.8	0.662326	$1.61 \times 10^{-4}$	0.679286	$2.75 \times 10^{-6}$	0.679852	$7.35 \times 10^{-7}$	0.664033	$2.77 \times 10^{-8}$
1.0	0.692351	$4.63 \times 10^{-4}$	0.727693	$3.28 \times 10^{-5}$	0.750727	$1.49 \times 10^{-6}$	0.761592	$5.38 \times 10^{-8}$

**Example 6.2.** Consider the following HF-FDE as [41]:

$$D^{\nu,\gamma,\varphi} R(t) = 2R(t) - R^2(t) + 1, \tag{6.2}$$

with the initial conditions

$$\begin{cases} R(0) = 0, & \gamma = 0, \\ I^{(1-\gamma)(1-\nu),\varphi} R(t)|_{t=0} = 0, & 0 < \gamma < 1. \end{cases}$$



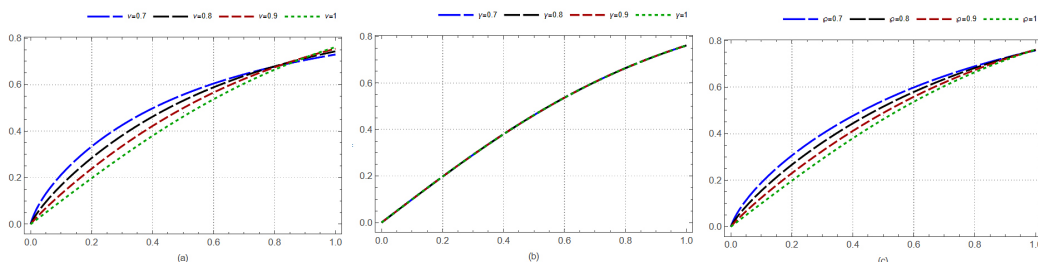


FIGURE 1. Diagrams of  $R(t)$  for (a) :  $\gamma = \wp = 1$ ; (b) :  $\nu = \wp = 1$ ; (c) :  $\nu = \gamma = 1$  with  $M = 7, \lambda = \frac{1}{2}$  (Example 6.1).

The exact solution of the classical model is  $R(t) = 1 + \sqrt{2}Tanh(\sqrt{2}t + \frac{1}{2} \log \frac{\sqrt{2}-1}{\sqrt{2}+1})$ . The comparison of the AE between suggested approach with variational iteration method (VIM) [7], optimal homotopy asymptotic method (OHAM) [24], modified homotopy perturbation method (MHPM) [29] and iterative reproducing kernel Hilbert spaces method (IRKHSM) [39] are shown in Table 4. As observed, the results presented in Table 4 demonstrate the efficiency and effectiveness of the presented scheme in comparison to other approaches. Also, we compare the NRs of our method with IRKHSM, reproducing kernel method (RKM) [23], MHPM, LOM, and Bernstein polynomials method (BPM) [48] for  $\nu = 0.75$  and  $\nu = 0.90$  in Tables 5 and 6, respectively. The NRs and REs for  $\lambda = \frac{1}{2}, M = 7$ , and varied values of  $\nu, \gamma, \wp$  are listed in Table 7. Additionally, Figure 2 illustrates the numerical solutions of  $R(t)$  for varied values of  $\nu, \gamma, \wp$ .

TABLE 4. The AEs for  $\nu = \gamma = \wp = 1, \lambda = 1$ , and varied values of  $M$  (Example 6.2).

$t$	VIM	OHAM	MHPM	IRKHSM	Presented method		
					$M = 9$	$M = 11$	$M = 13$
0.2	$1.03 \times 10^{-6}$	$2.90 \times 10^{-4}$	$1.20 \times 10^{-5}$	$9.23 \times 10^{-5}$	$1.38 \times 10^{-9}$	$9.54 \times 10^{-10}$	$3.94 \times 10^{-13}$
0.4	$3.33 \times 10^{-5}$	$2.50 \times 10^{-3}$	$3.03 \times 10^{-4}$	$7.35 \times 10^{-5}$	$4.94 \times 10^{-8}$	$5.96 \times 10^{-10}$	$3.12 \times 10^{-12}$
0.5	$7.26 \times 10^{-5}$	$4.40 \times 10^{-3}$	$1.55 \times 10^{-3}$	$7.62 \times 10^{-5}$	$7.75 \times 10^{-9}$	$3.44 \times 10^{-10}$	$1.44 \times 10^{-11}$
0.6	$9.98 \times 10^{-5}$	$5.50 \times 10^{-3}$	$4.69 \times 10^{-3}$	$7.56 \times 10^{-5}$	$7.50 \times 10^{-8}$	$1.12 \times 10^{-9}$	$7.60 \times 10^{-12}$
0.8	$1.54 \times 10^{-5}$	$3.80 \times 10^{-3}$	$1.88 \times 10^{-2}$	$3.94 \times 10^{-5}$	$5.83 \times 10^{-8}$	$3.65 \times 10^{-9}$	$4.61 \times 10^{-12}$
1.0	$3.47 \times 10^{-3}$	$3.40 \times 10^{-3}$	$3.43 \times 10^{-2}$	$7.12 \times 10^{-5}$	$1.14 \times 10^{-13}$	$1.02 \times 10^{-12}$	$1.92 \times 10^{-11}$

TABLE 5. The NRs and REs for  $\nu = 0.75$  with  $\gamma = \wp = 1, \lambda = \frac{1}{2}, M = 8$  (Example 6.2).

$t$	IRKHSM	RKM	MHPM	LOM	Presented method	
					NRs	REs
0.2	0.473076	0.469516	0.428892	0.3141626547	0.4735031278	$2.65 \times 10^{-5}$
0.4	0.936880	0.933596	0.891404	0.6948840414	0.9370150647	$8.92 \times 10^{-6}$
0.5	1.147576	1.144880	1.132763	0.9109355150	1.1476933146	$7.29 \times 10^{-11}$
0.6	1.333068	1.330980	1.370240	1.1600920300	1.3331549500	$2.34 \times 10^{-5}$
0.8	1.622033	1.621530	1.794879	1.5192229000	1.6221711080	$3.72 \times 10^{-6}$
1.0	1.817550	1.818650	2.087384	1.8110290000	1.8179655852	$5.97 \times 10^{-5}$

**Example 6.3.** Consider the following HF-FDE as [41]:

$$D^{\nu, \gamma, \wp} R(t) = -R(t), \tag{6.3}$$

with the initial conditions



TABLE 6. The NRs and REs for  $\nu = 0.90$  with  $\gamma = \varphi = 1, \lambda = \frac{1}{2}, M = 8$  (Example 6.2).

$t$	<i>IRKHSM</i>	<i>RKM</i>	<i>BPM</i>	<i>LOM</i>	<i>Presented method</i>	
					<i>NRs</i>	<i>REs</i>
0.2	0.314571	0.312985	0.314869	0.3152541236	0.3141822543	$3.56 \times 10^{-5}$
0.4	0.697246	0.695357	0.697544	0.6974216000	0.6967232069	$9.83 \times 10^{-5}$
0.5	0.903363	0.901484	0.903695	0.9043248600	0.9028486855	$1.06 \times 10^{-11}$
0.6	1.107569	1.105760	1.107866	1.1060828000	1.1070617198	$5.60 \times 10^{-5}$
0.8	1.477434	1.476060	1.477707	1.4731964000	1.4770428919	$6.36 \times 10^{-6}$
1.0	1.765103	1.764170	1.764520	1.7623270000	1.7647907078	$8.67 \times 10^{-5}$

TABLE 7. The NRs and REs for  $\lambda = \frac{1}{2}, M = 7$ , and differing values of  $\nu, \gamma, \varphi$  (Example 6.2).

$t$	$\nu = \gamma = \varphi = 0.65$		$\nu = \gamma = \varphi = 0.75$		$\nu = \gamma = \varphi = 0.85$		$\nu = \gamma = \varphi = 0.95$	
	<i>NRs</i>	<i>REs</i>	<i>NRs</i>	<i>REs</i>	<i>NRs</i>	<i>REs</i>	<i>NRs</i>	<i>REs</i>
0.2	1.102260	$2.83 \times 10^{-3}$	0.743711	$8.44 \times 10^{-4}$	0.474588	$7.34 \times 10^{-4}$	0.304210	$1.02 \times 10^{-3}$
0.4	1.386790	$1.70 \times 10^{-4}$	1.161720	$3.72 \times 10^{-4}$	0.898931	$4.30 \times 10^{-5}$	0.667543	$5.34 \times 10^{-5}$
0.5	1.472590	$7.88 \times 10^{-4}$	1.315120	$1.58 \times 10^{-4}$	1.093020	$1.98 \times 10^{-4}$	0.864382	$2.33 \times 10^{-4}$
0.6	1.539390	$8.10 \times 10^{-5}$	1.440730	$1.53 \times 10^{-5}$	1.268640	$2.02 \times 10^{-5}$	1.061880	$2.03 \times 10^{-5}$
0.8	1.637380	$2.47 \times 10^{-4}$	1.629590	$4.34 \times 10^{-5}$	1.557700	$6.03 \times 10^{-5}$	1.430110	$4.58 \times 10^{-5}$
1.0	1.706490	$7.32 \times 10^{-4}$	1.760950	$1.25 \times 10^{-4}$	1.768800	$1.73 \times 10^{-4}$	1.730160	$9.06 \times 10^{-5}$

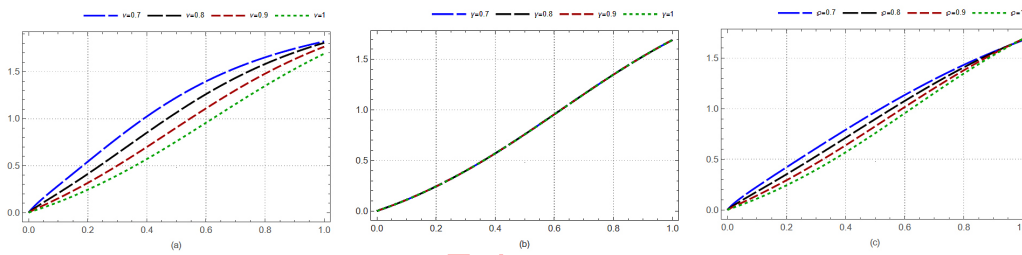


FIGURE 2. Diagrams of  $R(t)$  for (a) :  $\gamma = \varphi = 1$ ; (b) :  $\nu = \varphi = 1$ ; (c) :  $\nu = \gamma = 1$  with  $M = 7, \lambda = \frac{1}{2}$  (Example 6.2).

$$\begin{cases} R(0) = 1, & \gamma = 0, \\ I^{(1-\gamma)(1-\nu), \varphi} R(t)|_{t=0} = 1, & 0 < \gamma < 1. \end{cases}$$

The exact solution of the classical model is  $R(t) = e^{-t}$ . Table 8 presents the NRs and REs for  $\lambda = \frac{1}{2}, M = 8$ , and differing values of  $\nu, \gamma, \varphi$  obtained using the mentioned method. Also, Figure 3 shows diagrams of  $R(t)$  for diverse values of  $\nu, \gamma, \varphi$  with  $M = 8, \lambda = \frac{1}{2}$ .

TABLE 8. The NRs and REs for  $\lambda = \frac{1}{2}, M = 8$ , and differing values of  $\nu, \gamma, \varphi$  (Example 6.3).

$t$	$\nu = \gamma = \varphi = 0.75$		$\nu = \gamma = \varphi = 0.80$		$\nu = \gamma = \varphi = 0.85$		$\nu = \gamma = \varphi = 0.90$		$\nu = \gamma = \varphi = 0.95$	
	<i>NRs</i>	<i>REs</i>	<i>NRs</i>	<i>REs</i>	<i>NRs</i>	<i>REs</i>	<i>NRs</i>	<i>REs</i>	<i>NRs</i>	<i>REs</i>
0.2	0.655243	$1.53 \times 10^{-4}$	0.688632	$8.03 \times 10^{-5}$	0.722791	$3.87 \times 10^{-5}$	0.756494	$1.62 \times 10^{-5}$	0.818731	$3.84 \times 10^{-9}$
0.4	0.557234	$1.85 \times 10^{-4}$	0.574347	$9.13 \times 10^{-5}$	0.594883	$4.12 \times 10^{-5}$	0.618202	$1.62 \times 10^{-5}$	0.670320	$3.74 \times 10^{-9}$
0.5	0.523678	$1.22 \times 10^{-10}$	0.533739	$1.84 \times 10^{-11}$	0.547482	$1.82 \times 10^{-11}$	0.564519	$7.61 \times 10^{-12}$	0.606531	$4.40 \times 10^{-15}$
0.6	0.495784	$6.99 \times 10^{-5}$	0.499600	$3.32 \times 10^{-5}$	0.507053	$1.44 \times 10^{-5}$	0.517934	$5.44 \times 10^{-6}$	0.548812	$1.16 \times 10^{-9}$
0.8	0.451387	$6.26 \times 10^{-6}$	0.444722	$2.90 \times 10^{-6}$	0.441237	$1.23 \times 10^{-6}$	0.440884	$4.50 \times 10^{-7}$	0.449329	$8.62 \times 10^{-11}$
1.0	0.416977	$7.46 \times 10^{-5}$	0.401991	$3.39 \times 10^{-5}$	0.389606	$1.41 \times 10^{-5}$	0.379792	$5.06 \times 10^{-6}$	0.367879	$8.47 \times 10^{-10}$



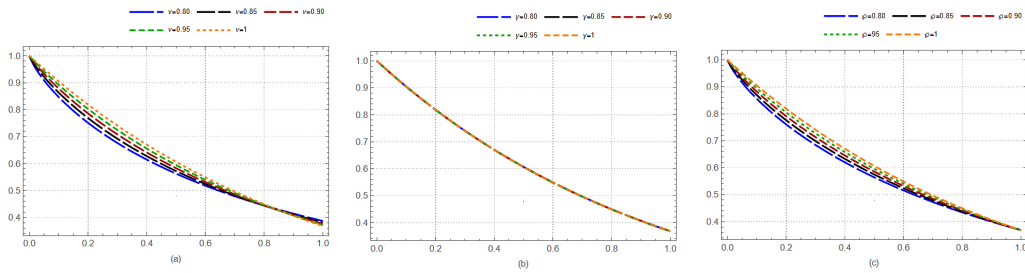


FIGURE 3. Diagrams of  $R(t)$  for (a) :  $\gamma = \varphi = 1$ ; (b) :  $\nu = \varphi = 1$ ; (c) :  $\nu = \gamma = 1$  with  $M = 8, \lambda = \frac{1}{2}$  (Example 6.3).

**Example 6.4.** Consider the following HF-FDE system as [41]:

$$\begin{cases} D^{\nu_1, \gamma, \varphi} R_1(t) = R_1(t) + R_2(t), \\ D^{\nu_2, \gamma, \varphi} R_2(t) = -R_1(t) + R_2(t), \end{cases} \tag{6.4}$$

with the initial conditions

$$\begin{cases} R_1(0) = 0, R_2(0) = 1, & \gamma = 0, \\ I^{(1-\gamma)(1-\nu), \varphi} R_1(t)|_{t=0} = 0, I^{(1-\gamma)(1-\nu), \varphi} R_2(t)|_{t=0} = 1, & 0 < \gamma < 1. \end{cases}$$

The exact solution of the classical model is  $R_1(t) = e^t \sin(t), R_2(t) = e^t \cos(t)$ . The NRs and AEs for the classical model with  $\lambda = 1, M = 11$  are reported in Table 9. The NRs and REs for  $\nu_1 = 0.70, \nu_2 = 0.90, \lambda = \frac{1}{2}, M = 8$ , and diverse values of  $\gamma, \varphi$  are discussed in Table 10. Figures 4 and 5 show the behavior of  $R_1(t)$ , and  $R_2(t)$  for diverse values of  $\nu, \gamma, \varphi$  with  $M = 8, \lambda = \frac{1}{2}$ .

TABLE 9. The NRs and AEs for  $\nu = \gamma = \varphi = 1$  and  $\lambda = 1, M = 11$  (Example 6.4).

$t$	$R_1(t)$			$R_2(t)$		
	Exact solution	NRs	AEs	Exact solution	NRs	AEs
0.1	0.1103329887	0.1103329887	$6.39 \times 10^{-16}$	1.0996496670	1.0996496680	0
0.2	0.2426552686	0.2426552686	$8.88 \times 10^{-16}$	1.1970560214	1.1970560214	$4.44 \times 10^{-16}$
0.3	0.3989105538	0.3989105538	$9.43 \times 10^{-16}$	1.2895693740	1.2895693740	$2.22 \times 10^{-16}$
0.4	0.5809439008	0.5809439008	$6.66 \times 10^{-16}$	1.3740615389	1.3740615389	0
0.5	0.7904390832	0.7904390832	$1.11 \times 10^{-16}$	1.4468890366	1.4468890366	$2.22 \times 10^{-16}$
0.6	1.0288456663	1.0288456663	$6.66 \times 10^{-16}$	1.5038595406	1.5038595406	0
0.7	1.2972951119	1.2972951119	$8.88 \times 10^{-16}$	1.5402030254	1.5402030254	$6.66 \times 10^{-16}$
0.8	1.5965053406	1.5965053406	$8.88 \times 10^{-16}$	1.5505492968	1.5505492968	0
0.9	1.9266733040	1.9266733040	$1.11 \times 10^{-15}$	1.5289138119	1.5289138119	$2.22 \times 10^{-16}$
1.0	2.2873552872	2.2873552872	0	1.4686939399	1.4686939399	0

TABLE 10. The NRs and REs for  $\nu_1 = 0.70, \nu_2 = 0.90, \lambda = \frac{1}{2}, M = 8$ , and differing values of  $\gamma, \varphi$  (Example 6.4).

$t$	$\gamma = \varphi = 0.85$			$\gamma = \varphi = 0.90$			$\gamma = \varphi = 0.95$		
	NRs( $R_1(t)$ )	NRs( $R_2(t)$ )	REs	NRs( $R_1(t)$ )	NRs( $R_2(t)$ )	REs	NRs( $R_1(t)$ )	NRs( $R_2(t)$ )	REs
0.2	0.68260	1.23326	$9.22 \times 10^{-5}$	0.62061	1.22448	$6.89 \times 10^{-5}$	0.56439	1.21457	$5.03 \times 10^{-5}$
0.4	1.24328	1.27929	$9.82 \times 10^{-5}$	1.17801	1.28635	$7.11 \times 10^{-5}$	1.11534	1.29053	$5.01 \times 10^{-5}$
0.5	1.52593	1.25329	$1.90 \times 10^{-10}$	1.46936	1.26787	$3.64 \times 10^{-11}$	1.41346	1.27950	$1.82 \times 10^{-11}$
0.6	1.80888	1.19454	$3.36 \times 10^{-5}$	1.76691	1.21428	$7.80 \times 10^{-6}$	1.72393	1.23143	$1.64 \times 10^{-5}$
0.8	2.36507	0.97559	$2.77 \times 10^{-6}$	2.36660	0.99325	$1.93 \times 10^{-6}$	2.36538	1.00945	$1.31 \times 10^{-6}$
1.0	2.88592	0.61610	$3.07 \times 10^{-5}$	2.94228	0.60699	$2.10 \times 10^{-5}$	2.99656	0.59627	$1.40 \times 10^{-5}$



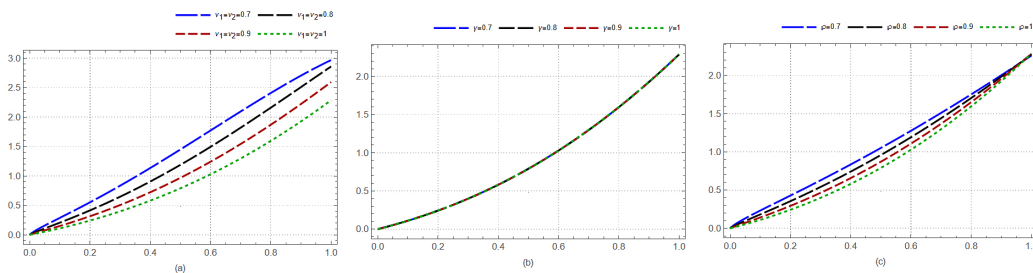


FIGURE 4. Diagrams of  $R_1(t)$  for (a) :  $\gamma = \varphi = 1$ ; (b) :  $\nu_1 = \nu_2 = \varphi = 1$ ; (c) :  $\nu_1 = \nu_2 = \gamma = 1$  with  $M = 8, \lambda = \frac{1}{2}$  (Example 6.4).

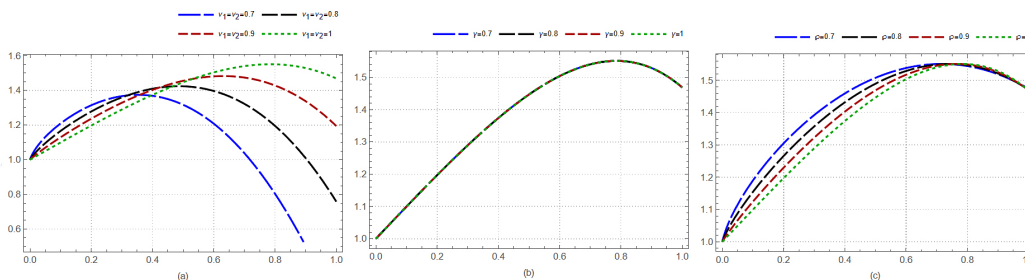


FIGURE 5. Diagrams of  $R_2(t)$  for (a) :  $\gamma = \varphi = 1$ ; (b) :  $\nu_1 = \nu_2 = \varphi = 1$ ; (c) :  $\nu_1 = \nu_2 = \gamma = 1$  with  $M = 8, \lambda = \frac{1}{2}$  (Example 6.4).

**Example 6.5.** Consider the following HF-FDE as [41]:

$$D^{\nu_3, \gamma, \varphi} R(t) = -{}^C D^{\nu_1} R(t) + 2{}^C D^{\nu_2} R(t) - R(t) + t^3 - 6t^2 + 6t + \frac{16}{5\sqrt{\pi}} t^{2.5}, \tag{6.5}$$

with the initial conditions

$$\begin{cases} R(0) = R'(0) = 0, & \gamma = 0, \\ I^{(1-\gamma)(1-\nu), \varphi} R(t)|_{t=0} = R'(0) = 0, & 0 < \gamma < 1. \end{cases}$$

The exact solution for  $\nu_1 = 2, \nu_2 = 1, \nu_3 = 0.5$  is  $R(t) = t^3$ . We compare the NRs and REs for  $\nu_1 = 2, \nu_2 = 1, \nu_3 = 0.5$ , with different values of  $\lambda$  in Table 11. In fact, this table shows the effect of parameter  $\lambda$ . The NRs and REs for  $\lambda = \frac{1}{2}, M = 10, \nu_1 = 2, \nu_2 = 1, \nu_3 = 0.5$ , and diverse values of  $\gamma, \varphi$  are displayed in Table 12. To further analyze, we plot the approximate solutions of  $R(t)$  for  $\nu_1 = 2, \nu_2 = 1, \nu_3 = 0.5$  with different values of  $\varphi, \gamma$  in Figure 6.

TABLE 11. The NRs and REs for  $\nu_1 = 2, \nu_2 = 1, \nu_3 = 0.5$ , and  $\gamma = \varphi = 1$  (Example 6.5).

$t$	$M = 2$				$M = 4$			
	$\lambda = \frac{1}{4}$	$\lambda = \frac{1}{2}$	$\lambda = \frac{2}{3}$	$\lambda = 1$	$\lambda = \frac{1}{4}$	$\lambda = \frac{1}{2}$	$\lambda = \frac{2}{3}$	$\lambda = 1$
0.2	$1.31 \times 10^{-2}$	$6.94 \times 10^{-17}$	$1.51 \times 10^{-3}$	$5.20 \times 10^{-18}$	$8.62 \times 10^{-16}$	$2.78 \times 10^{-17}$	$1.10 \times 10^{-4}$	$8.67 \times 10^{-18}$
0.4	$2.94 \times 10^{-2}$	$8.33 \times 10^{-17}$	$3.10 \times 10^{-3}$	$1.39 \times 10^{-17}$	$1.68 \times 10^{-15}$	0	$2.24 \times 10^{-4}$	$2.78 \times 10^{-17}$
0.5	$3.83 \times 10^{-2}$	$6.94 \times 10^{-17}$	$3.81 \times 10^{-3}$	0	$1.97 \times 10^{-15}$	$4.16 \times 10^{-17}$	$2.98 \times 10^{-4}$	$2.78 \times 10^{-17}$
0.6	$4.79 \times 10^{-2}$	$2.78 \times 10^{-17}$	$4.56 \times 10^{-3}$	0	$2.14 \times 10^{-15}$	$8.33 \times 10^{-17}$	$3.81 \times 10^{-4}$	$5.55 \times 10^{-17}$
0.8	$7.01 \times 10^{-2}$	$1.11 \times 10^{-16}$	$6.42 \times 10^{-3}$	$1.11 \times 10^{-16}$	$1.67 \times 10^{-15}$	$2.22 \times 10^{-16}$	$5.59 \times 10^{-4}$	0
1.0	$9.55 \times 10^{-2}$	$3.33 \times 10^{-16}$	$8.66 \times 10^{-3}$	0	$2.22 \times 10^{-16}$	$4.44 \times 10^{-16}$	$7.60 \times 10^{-4}$	0



TABLE 12. The NRs and REs for  $\lambda = \frac{1}{2}, M = 10, \nu_1 = 2, \nu_2 = 1, \nu_3 = 0.5$ , and diverse values of  $\gamma, \wp$  (Example 6.5).

$t$	$\gamma = \wp = 0.50$		$\gamma = \wp = 0.60$		$\gamma = \wp = 0.70$		$\gamma = \wp = 0.80$		$\gamma = \wp = 0.90$	
	NRs	REs	NRs	REs	NRs	REs	NRs	REs	NRs	REs
0.0	0	$1.04 \times 10^{-2}$	0	$2.22 \times 10^{-3}$	0	$2.08 \times 10^{-5}$	0	$3.33 \times 10^{-4}$	0	$1.93 \times 10^{-4}$
0.2	0.008023	$2.69 \times 10^{-6}$	0.008024	$6.55 \times 10^{-7}$	0.008021	$7.02 \times 10^{-8}$	0.008016	$4.95 \times 10^{-8}$	0.008009	$3.60 \times 10^{-8}$
0.4	0.064022	$3.51 \times 10^{-7}$	0.064116	$9.03 \times 10^{-8}$	0.064145	$1.27 \times 10^{-8}$	0.064130	$4.62 \times 10^{-9}$	0.064080	$4.03 \times 10^{-9}$
0.5	0.124398	$2.21 \times 10^{-11}$	0.124816	$1.03 \times 10^{-13}$	0.125033	$9.93 \times 10^{-13}$	0.125116	$1.88 \times 10^{-12}$	0.125100	$9.10 \times 10^{-15}$
0.6	0.213196	$1.13 \times 10^{-7}$	0.214521	$3.03 \times 10^{-8}$	0.215322	$4.96 \times 10^{-9}$	0.215778	$1.03 \times 10^{-9}$	0.215985	$1.14 \times 10^{-9}$
0.8	0.491888	$6.52 \times 10^{-8}$	0.499424	$1.81 \times 10^{-8}$	0.504521	$3.30 \times 10^{-9}$	0.508029	$3.78 \times 10^{-10}$	0.510426	$5.81 \times 10^{-10}$
1.0	0.920136	$1.37 \times 10^{-7}$	0.947617	$3.92 \times 10^{-8}$	0.967128	$7.75 \times 10^{-9}$	0.981407	$3.95 \times 10^{-10}$	0.992038	$1.08 \times 10^{-9}$

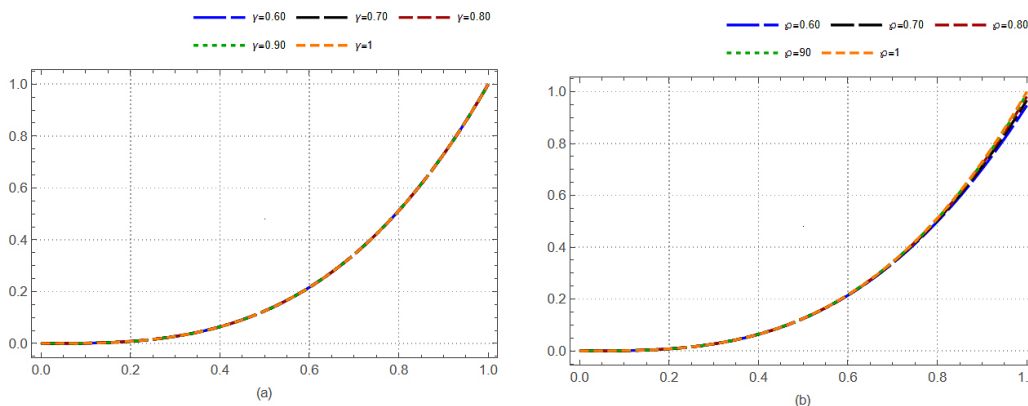


FIGURE 6. Diagrams of  $R(t)$  for  $\nu_1 = 2, \nu_2 = 1, \nu_3 = 0.5$  with (a) :  $\wp = 1$ ; (b) :  $\gamma = 1$  with  $M = 9, \lambda = \frac{1}{2}$  (Example 6.5).

### 7. CONCLUSIONS

The constants in this research, including the fractional order  $\nu$ , the type of Hilfer derivative  $\gamma$ , and the fractal parameter  $\wp$ , can be adjusted to analyze the behavior of various problems and achieve the best outcomes for each case. To approximate the solution of HF-FEs, we introduced the FCFs and their properties. The problem is then approximately solved using the FCFs, collocation method, and Newton’s iterative approach to handle the resulting system of equations. The solutions obtained using the proposed method indicate that the best value of  $\lambda$  for the classical model ( $\nu = \gamma = \wp = 1$ ) is  $\lambda = 1$ , and for non-classical models is  $\lambda = \frac{1}{2}$ . A small number of the FCFs is sufficient to achieve a satisfactory result; thus, the approximation using the FCFs requires a short CPU time. Examples with satisfactory results are provided to illustrate the applications of this scheme. This technique can be applied to solve other FDEs with different concepts that arise from physical models. We plan to do the following works in the future:

- This method can be used to solve different problems such as fractional partial differential equations, two-dimensional fractional optimal control problems, fractal-fractional differential equations, stochastic differential equations, inverse problems, etc.
- Wavelets can be combined with the deep neural network method and the parallel least-squares support vector machine method for solving the proposed problems.
- Examining existence and uniqueness of the solution for the proposed Hilfer fractal-fractional differential equations.
- Stability analysis of the suggested scheme for the numerical approximation of the problem under study is an interesting problem for future works.



**Author Contributions.** **Parisa Rahimkhani:** Conceptualization, Data curation, Investigation, Software, Writing -original draft.

**Nasrin Samadyar:** Conceptualization, Data curation, Investigation, Software, Writing -original draft.

**Mohsen Razzaghi:** Conceptualization, Validation, and editing.

**Data availability statement.** Data will be made available on reasonable request.

**Funding.** The authors received no financial support for the research, authorship, and publication of this paper.

**Declaration of Competing Interest.** The authors declare that they have no known competing financial interests or personal relationships that could have appeared to influence the work reported in this paper.

**Acknowledgments.** We express our sincere thanks to the anonymous referees for valuable suggestions that improved the paper.

#### REFERENCES

- [1] T. Abdeljawad and D. Baleanu, *Integration by parts and its applications of a new nonlocal fractional derivative with Mittag-Leffler nonsingular kernel*, arXiv preprint arXiv, (2016), 1607.00262.
- [2] W. Adel and K. Srinivasa, *A new clique polynomial approach for fractional partial differential equations*, International Journal of Nonlinear Sciences and Numerical Simulation, *24*(8) (2024), 2839–2851.
- [3] B. Agheli, *Approximate solution for solving fractional Riccati differential equations via trigonometric basic functions*, Trans. A. Razmadze Math. Inst., *172*(3) (2018), 299–308.
- [4] M. A. Almalahi, M. S. Abdo, and S. K. Panchal, *Periodic boundary value problems for fractional implicit differential equations involving Hilfer fractional derivative*, *9*(2) (2020), 16–44.
- [5] A. Atangana, *Fractal-fractional differentiation and integration: connecting fractal calculus and fractional calculus to predict complex system*, Chaos Solitons Fractals, *102* (2017), 396–406.
- [6] A. Atangana and S. Qureshi, *Modeling attractors of chaotic dynamical systems with fractal-fractional operators*, Chaos Solitons Fractals, *123* (2019), 320–337.
- [7] B. Batiha, M. S. M. Noorani, and I. Hashim, *Application of variational iteration method to a general Riccati equation*, Int. Math. Forum, *2* (2007), 2759–2770.
- [8] P. Bedi, A. Kumar, T. Abdeljawad, and A. Khan, *Study of Hilfer fractional evolution equations by the properties of controllability and stability*, Alex. Eng. J., *60*(4) (2021), 3741–3749.
- [9] R. M. Ganji, H. Jafari, M. Kgarose, and A. Mohammadi, *Numerical solutions of time fractional Klein-Gordon equations by clique polynomials*, Alexandria Engineering Journal, *60* (2021), 4563–4571.
- [10] Z. Gao and X. Yu, *Existence results for BVP of a class of Hilfer fractional differential equations*, J. Appl. Math. Comput., *56* (2018), 217–233.
- [11] H. Hassani, J. T. Machado, Z. Avazzadeh, E. Naraghirad, and M. S. Dahaghin, *Generalized Bernoulli polynomials: solving nonlinear 2D fractional optimal control problems*, J. Sci. Comput., *83* (2020), 1–21.
- [12] M. H. Heydari, A. Atangana, Z. Avazzadeh, and Y. Yang, *Numerical treatment of the strongly coupled nonlinear fractal-fractional Schrödinger equations through the shifted Chebyshev cardinal functions*, Math. Meth. Appl. Sci., *59*(4) (2020), 2037–2052.
- [13] M. H. Heydari, Z. Avazzadeh, and A. Atangana, *Shifted Vieta-Fibonacci polynomials for the fractal-fractional fifth-order KdV equation*, Math. Meth. Appl. Sci., *44* (2021), 6716–6730.
- [14] M. H. Heydari and M. Razzaghi, *Highly accurate solutions for space-time fractional Schrödinger equations with a non-smooth continuous solution using the hybrid clique functions*, Mathematical Sciences, *17*(1) (2023), 31–42.
- [15] M. H. Heydari and M. Razzaghi, *Jacobi polynomials method for a coupled system of Hadamard fractional Klein-Gordon-Schrödinger equations*, Alexandria Engineering Journal, (2024), 73–86.
- [16] R. Hilfer, *Applications of fractional calculus in physics*, World Scientific, Singapore, 2000.
- [17] C. Hoede, *Hard graphs for the maximum clique problem*, Discr. Mat., *72* (1988), 175–179.



- [18] C. Hoede and X. Li, *Clique polynomials and independent set polynomials of graphs*, *Discr. Math.*, *125* (1994), 219–228.
- [19] L. L. Huang, D. Baleanu, Z. W. Mo, and G. Ch. Wu, *Fractional discrete-time diffusion equation with uncertainty: applications of fuzzy discrete fractional calculus*, *Phys. A, Stat. Mech. Appl.*, *508* (2018), 166–175.
- [20] M. Izadi, and H. M. Srivastava, *Fractional clique collocation technique for numerical simulations of fractional-order Brusselator chemical model*, *Axioms*, *11*(11) (2022), 654.
- [21] S. Kumbinarasaiah and K. R. Raghunatha, *Study of special types of boundary layer natural convection flow problems through the clique polynomial method*, *Heat Transfer.*, *51*(10) (2022), 434–450.
- [22] S. Kumbinarasaiah, H. S. Ramane, K. S. Pise, and G. Hariharan, *Numerical solution for nonlinear Klein-Gordon equation via operational matrix by clique polynomial of complete graphs*, *International Journal of Applied and Computational Mathematics*, *7*(12) (2021), 1–19.
- [23] X. Y. Li, B. Y. Wu, and R. T. Wang, *Reproducing kernel method for fractional Riccati differential equations*, *Abstr. Appl. Anal.*, *2014* (2014), Article ID 970967.
- [24] F. Mabood, A. I. Ismail, and I. Hashim, *Application of optimal homotopy asymptotic method for the approximate solution of Riccati equation*, *Sains Malays*, *42* (2013), 863–867.
- [25] F. Mirzaee and S. F. Hoseini, *Hybrid functions of Bernstein polynomials and block-pulse functions for solving optimal control of the nonlinear Volterra integral equations*, *Indag Math.*, *27*(3) (2016), 835–849.
- [26] A. N. Nirmala and S. Kumbinarasaiah, *A new graph theoretic analytical method for nonlinear distributed order fractional ordinary differential equations by clique polynomial of cocktail party graph*, *Journal of Umm Al-Qura University for Applied Sciences*, *10* (2024), 445–456.
- [27] A. N. Nirmala and S. Kumbinarasaiah, *A novel analytical method for the multi-delay fractional differential equations through the matrix of clique polynomials of the cocktail party graph*, *Results in Control and Optimization*, *12* (2023), 100280.
- [28] H. T. B. Ngo, T. N. Vo, and M. Razzaghi, *An effective method for solving nonlinear fractional differential equations*, *Engineering with Computers*, *38* (2022), 207–218.
- [29] Z. Odibat and S. Momani, *Modified homotopy perturbation method: application to quadratic Riccati differential equation of fractional order*, *Chaos Solitons Fractals*, *36*(1) (2008), 167–174.
- [30] Y. Ordokhani, S. Sabermahani, and P. Rahimkhani, *Application of Chelyshkov wavelets and least squares support vector regression to solve fractional differential equations arising in optics and engineering*, *Mathematical Methods in the Applied Sciences*, *48*(2) (2025), 1996–2010.
- [31] P. Rahimkhani, *A numerical method for  $\psi$ -fractional integro-differential equations by Bell polynomials*, *Applied Numerical Mathematics*, *207* (2025), 244–253.
- [32] P. Rahimkhani and M. H. Heydari, *Fractional shifted Morgan-Voyce neural networks for solving fractal-fractional pantograph differential equations*, *Chaos, Solitons and Fractals*, *175* (2023), 114070.
- [33] P. Rahimkhani and M. H. Heydari, *Numerical investigation of  $\psi$ -fractional differential equations using wavelets neural networks*, *Computational and Applied Mathematics*, *44*(1) (2025), 54.
- [34] P. Rahimkhani, Y. Ordokhani, and E. Babolian, *Fractional-order Bernoulli wavelets and their applications*, *Appl. Math. Modell.*, *40* (2016), 8087–8107.
- [35] P. Rahimkhani, Y. Ordokhani, and S. Sabermahani, *Numerical solution of fractal-fractional differential equations system via Vieta-Fibonacci polynomials fractal-fractional integral operators*, *International Journal of Numerical Modelling: Electronic Networks, Devices and Fields - Decision*, *37*(5) (2024), e3283.
- [36] P. Rahimkhani, Y. Ordokhani, and S. Sedaghat, *The numerical treatment of fractal-fractional 2D optimal control problems by Müntz-Legendre polynomials*, *Optimal Control, Applications and Methods*, *44*(6) (2023) 3033–3051.
- [37] A. Rayal and S. R. Verma, *Numerical analysis of pantograph differential equation of the stretched type associated with fractal-fractional derivatives via fractional order Legendre wavelets*, *Chaos, Solitons and Fractals*, *139* (2020), 110076.
- [38] S. Sabermahani, Y. Ordokhani, and P. Rahimkhani, *Application of generalized Lucas wavelet method for solving nonlinear fractal-fractional optimal control problems*, *Chaos, Solitons and Fractals*, *170* (2023), 113348.



- [39] M. G. Sakar, A. Akgül, and D. Baleanu, *On solutions of fractional Riccati differential equations*, Advances in Difference Equations, *2017* (2017), 1–10.
- [40] S. Shafipour and R. Katani, *Convergence analysis for piecewise Lagrange interpolation method of fractal fractional model of tumor-immune interaction with two different kernels*, Computational Methods for Differential Equations, *13*(1) (2024), 169–82.
- [41] A. M. Shloof, N. Senua, A. Ahmadiand, N. M. A. NikLonga, and S. Salahshourf, *Solving fractal-fractional differential equations using operational matrix of derivatives via Hilfer fractal-fractional derivative sense*, Appl. Numer. Math. *178* (2022 ), 386–403.
- [42] H. M. Srivastava and K. M. Saad, *Numerical simulation of the fractal-fractional Ebola virus*, Fractal Fract., *4*(4) (2020), 1–13
- [43] H. Sun, W. Chen, C. Li, and Y. Chen, *Finite difference schemes for variable-order time fractional diffusion equation*, Int. J. Bifurc. Chaos., *22*(04) (2012), 1250085.
- [44] H. Sweis, O. A. Arqub, and N. Shawagfeh, *Hilfer fractional delay differential equations: existence and uniqueness computational results and pointwise approximation utilizing the shifted Legendre Galerkin algorithm*, Alexandria Engineering Journal, *81* (2023), 548–559.
- [45] D. Vivek, K. Kanagarajan, and E. M. Elsayed, *Some existence and stability results for Hilfer fractional implicit differential equations with nonlocal conditions*, Mediterr. J. Math. *15* (2018), 1–21.
- [46] W. Wang, and M. A. Khan, *Analysis and numerical simulation of fractional model of bank data with fractal-fractional Atangana-Baleanu derivative*, Journal of Computational and Applied Mathematics, *369* (2020), 112646.
- [47] J. Wang, and Y. Zhang, *Nonlocal initial value problems for differential equations with Hilfer fractional derivative*, Appl. Math. Comput., *266* (2015), 850–859.
- [48] S. Yüzbaşı, *Numerical solutions of fractional Riccati type differential equations by means of the Bernstein polynomials*, Appl. Math. Comput., *219* (2013), 6328–6343.
- [49] S. Zerbib, Kh. Hilal, and A. Kajoun, *On the non-local  $\varphi$ -Hilfer hybrid fractional differential equations: an existence study*, Computational Methods for Differential Equations, (2025).
- [50] C. J. Zúñiga-Aguilar, J. F. Gómez-Aguilar, H. M. Romero-Ugalde, R. F. Escobar-Jiménez, G. Fernández-Anaya, and F. E. Alsaadi, *Numerical solution of fractal-fractional Mittag-Leffler differential equations with variable-order using artificial neural networks*, Engineering with Computers, *38* (2022), 2669–2682.

